Dalton Transactions

Accepted Manuscript

ROYAL SOCIETY OF CHEMISTRY

www.rsc.org/dalton

Journal Name

RSCPublishing

ARTICLE

Recyclable Chemosensor for Oxalate Based on Bimetallic Complexes of a Dinucleating Bis(iminopyridine) Ligand

Cite this: DOI: 10.1039/x0xx00000x

Received 00th January 2012,
Accepted 00th January 2012

DOI: 10.1039/x0xx00000x

www.rsc.org/

J. W. Beattie,[a] D. S. White,[a] A. Bheemaraju,[a] P. D. Martin,[a] and S. Groysman[a*]

Herein we describe bimetallic di-nickel and di-copper complexes $[Ni_2(L)Br_4]$ (**1**) and $[Cu_2(L)Br_4(NCMe)_2]$ (**2**) (L = (1*E*,1'*E*)-N,N'-(1,4-phenylenebis(methylene))bis(1-(6-(2,4,6-triisopropylphenyl)pyridin-2-yl)methanimine)) that bind oxalate intramolecularly to form $[Ni_2(L)Br_2(C_2O_4)(NCMe)]$ (**3**) and $[Cu_2(L)Br_2(C_2O_4)]$ (**4**). For the di-nickel complex **1**, oxalate incorporation is accompanied by a significant colour change, from red-pink (**1**) to deep green (**3**). Mass spectrometric experiments demonstrate that the compound **1** is selective for oxalate *versus* related mono- and di-carboxylates tested. Oxalate can be released by the addition of slight excess of calcium bromide that forms insoluble calcium oxalate and restores the original $Ni_2(L)Br_4$ species. The product of the oxalate release was crystallized as $[Ni_2(L)Br_4]\bullet CaBr_2(THF)_4$ species.

Introduction

Chemical detection of oxalate is of considerable interest due to the important roles that oxalate plays in food chemistry and in biological processes.[1] Oxalate is frequently encountered as a bridging ligand in transition metal chemistry.[2] Therefore, bimetallic complexes that are designed to bind oxalate intramolecularly can be envisioned as efficient oxalate sensors. The vast majority of bimetallic oxalate complexes feature intermolecular coordination of oxalate.[3] Several systems have been recently reported that bind oxalate intramolecularly.[4-8] The majority of these systems rely on fluorescence indicators. The design of a system that enables detection of oxalate without the use of fluorescence indicators[9, 10] and is also capable of regeneration is of considerable interest. Toward this end, we report bimetallic complexes that enable simple colourimetric detection of oxalate and can be easily recycled.

We and others are investigating bimetallic complexes for the cooperative binding and activation of small molecules.[11] We have recently reported a new family of dinucleating bis(iminopyridine) ligands linked by a para-xylylene bridge.[12] We hypothesized that the resulting bimetallic complexes possess an appropriate cavity size to bind oxalate between the two transition metals. Furthermore, we postulated that the highly flexible nature of the ligands will enable reversible binding of oxalate. For the current study, we chose ligand L featuring 2,4,6-triisopropylphenyl substituents in the *ortho* positions of the pyridine as its complexes demonstrated significantly better solubility than complexes of other bis(iminopyridine) ligands.[12c] In addition, we anticipated that the bulky groups in the 2' position will lead to the well-defined bimetallic species.[13] We focused on the nickel(II) and copper(II) metal centres since they are capable of binding oxalate, yet not oxophilic enough to prevent its removal.

Results and Discussion

Synthetic transformations described in this paper are summarized in **Figure 1**. To access di-nickel(II) and di-copper(II) complexes anticipated to serve as oxalate sensors, we treated one equivalent of the ligand L in tetrahydrofuran (THF) with two equivalents of the $NiBr_2$(dme) (dme = dimethoxyethane) or $CuBr_2$ in THF or THF/CH_3CN (CH_3CN = acetonitrile). The compounds $Ni_2(L)Br_4$ (**1**) and $Cu_2(L)Br_4$ (**2**) were obtained as pink (**1**) and green (**2**) crystals by vapour diffusion of ether into the saturated THF and CH_3CN solutions in 82% and 75% yields, respectively. Compounds **1** and **2** were characterized by ^{1}H NMR, solution magnetic measurements (using Evans method), elemental analysis, X-ray crystallography, IR spectroscopy, and mass spectrometry (see below). Well-resolved ^{1}H NMR spectrum of **1** (**Figure S3**) demonstrates five paramagnetically shifted signals (in the range of 10 – 77 ppm) that can be attributed to the five different types of aromatic protons of L. In contrast, the ^{1}H NMR spectrum of

2 is significantly less informative (**Figure S4**). Solution magnetic moment of **1** (determined by Evans method) is consistent with four unpaired electrons per molecule of 1 (μ_{obs} = 4.83 versus μ_{calc} = 4.90). For the di-copper complex 2, the solution magnetic moment was determined to be 2.16 (μ_{calc} = 2.83).

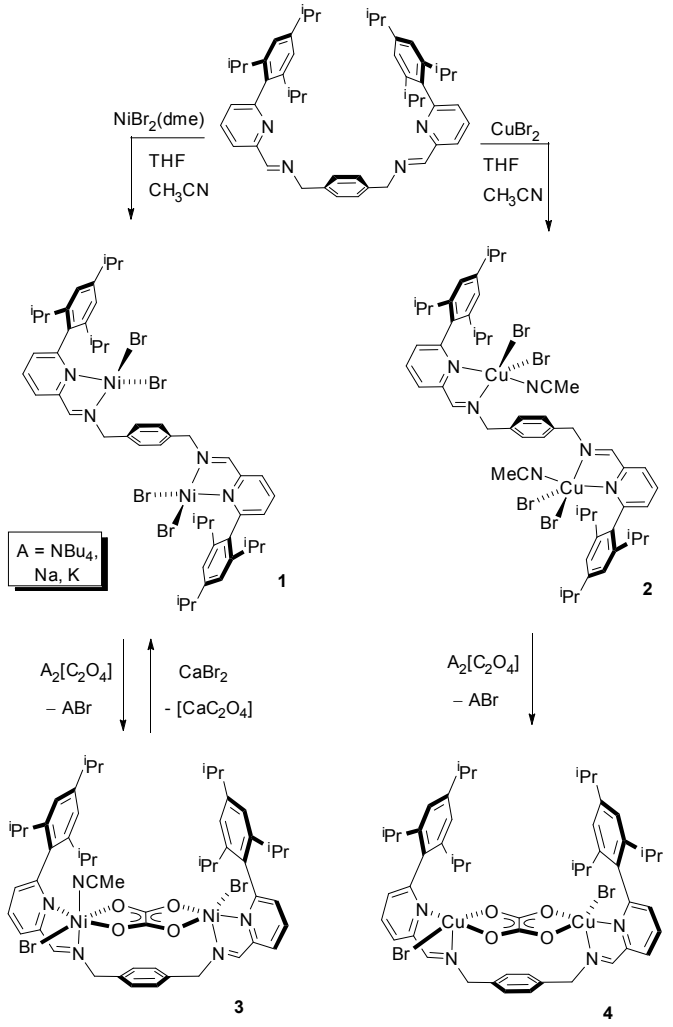

Figure 1. Synthesis of compounds **1** and **2** and their reactivity with oxalate salts to afford compounds **3** and **4**.

X-ray structures of compounds **1** and **2** are presented in **Figure 2**. X-ray structures of both complexes (see **Figure 2** for the structures of **1** and **2**) notably demonstrate *anti* geometry of the two sides of a complex. Accordingly, the compounds exhibit large metal – metal separations (Ni --- Ni is 11.309 Å, Cu --- Cu is 11.380 Å). Both compounds are centrosymmetric (space groups are $P2_1/c$ and P-1), so only half of the molecule constitutes an asymmetric unit. Whereas both compounds can be synthesized in the presence of CH_3CN, only the di-copper complex features CH_3CN binding to the metal centres. Accordingly, the di-copper complex **2** features distorted square-pyramidal geometry at the copper(II) centres, whereas the di-nickel complex **1** has four-coordinate metal centres. CH_3CN ligands bound to the copper centres are found in two alternate conformations; only one is shown for clarity.

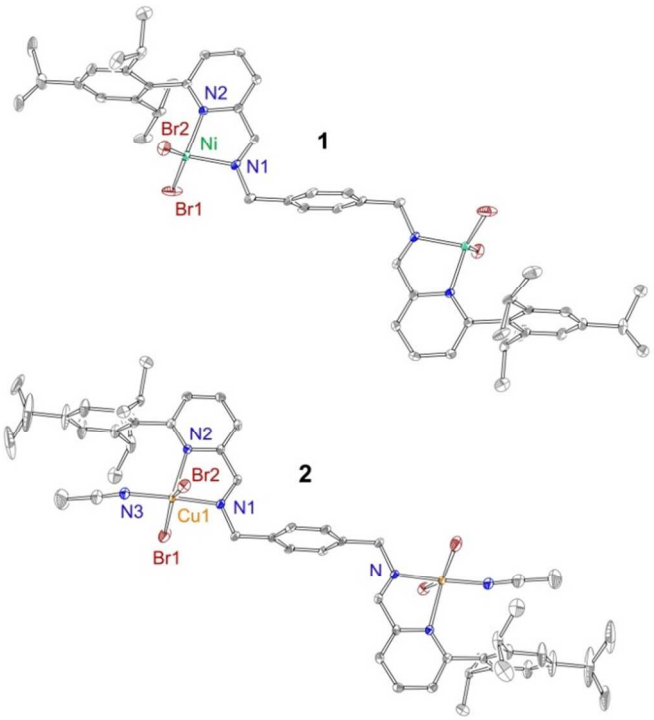

Figure 2. Structures of complexes **1** and **2**. Selected distances and angles for 1: Ni --- Ni 11.309(1) Å, Ni – Br1 2.312(1) Å, Ni – Br2 2.318(1) Å, Ni – N1 2.006(3) Å, Ni – N2 1.980(3) Å, Br1 – Ni – Br2 135.0(1) °, N1 – Ni – N2 82.9(1) °. Selected distances and angles for 2: Cu --- Cu 11.38(1) Å, Cu – Br1 2.474(1) Å, Cu – Br2 2.425(1) Å, Cu – N1 1.970(3) Å, Cu – N2 2.227(3) Å, Cu – N3 1.952(3) Å, Br1 – Cu – Br2 151.1(1) °, N1 – Cu – N2 79.2(1) °, N1 – Cu – N3 174.6 °.

Next, we investigated the reactivity of complexes **1** and **2** with oxalate. For the preliminary investigation, we synthesized $(NBu_4)_2[C_2O_4]$,[14] that is soluble in polar organic solvents (e.g. CH_3CN). The addition of one equivalent of $(NBu_4)_2[C_2O_4]$ in CH_3CN to the red-pink solution of **1** in THF immediately results in a colour change to green. Subsequent work-up and crystallization from CH_3CN/ether yielded green crystals of the oxalate-bridged complex $[Ni_2(L)Br_2(\mu_2\text{-}C_2O_4)(NCMe)]$ (**3**) in 78% yield. Similarly, the reaction of $(NBu_4)_2[C_2O_4]$ with bright yellow-green THF/CH_3CN solution of **2** yields dark green compound **4** (83% yield). Compounds **3** and **4** were also characterized by elemental analysis, X-ray crystallography, IR spectroscopy and mass spectrometry. As both **3** and **4** are only sparingly soluble in common deuterated solvents, we were not able to determine their solution magnetic moments reliably.

The X-ray structures of **3** and **4** are displayed in **Figure 3**. Both compounds demonstrate intramolecular binding of the oxalate, with the metal – metal distances being 5.36 Å for **3** and 5.20 Å for **4**, that are typical metal-metal separations in the intermolecular complexes of the corresponding metal-oxalate complexes.[5] Interestingly, the di-nickel complex **3** demonstrates two different coordination environments at the nickel centres.

Ni1 is hexa-coordinate, due to the coordinated CH_3CN ligand. Ni2 is penta-coordinate, featuring distorted square-pyramidal geometry. Both copper centers in **4** are penta-coordinate. However, they demonstrate two different coordination geometries, with Cu1 being approximately square pyramidal, and Cu2 being trigonal bipyramidal. For the selected bonds and angles, see **Figure 3** below. We have also characterized complexes **1-4** by IR spectroscopy (**Figure 4**). The complexes demonstrate very similar IR spectra with the notable exception of the strong peak around 1635 cm^{-1} associated with the oxalate stretch (1645 cm^{-1} in sodium oxalate).[15]

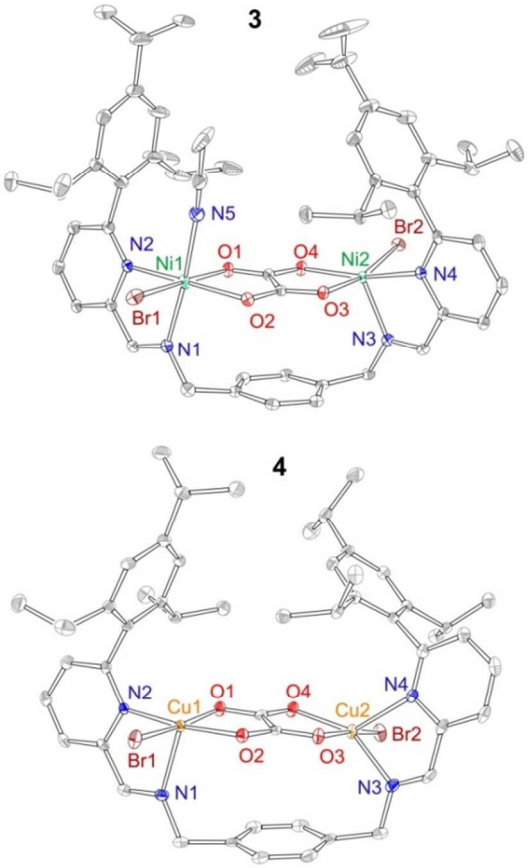

Figure 3. Structures of complexes **3** and **4**. Selected distances and angles for **3**: Ni1 --- Ni2 5.36 Å, Ni1 – Br1 2.516(1) Å, Ni2 – Br2 2.425(1) Å, Ni1 – N1 2.062(2) Å, Ni1 – N2 2.170(2) Å, Ni1 – N3 2.096(2) Å, Ni1 – O1 2.064(3) Å, Ni1 – O2 2.081(3) Å, Ni2 – N3 2.033(2) Å, Ni2 – N4 2.095(2) Å, Ni2 – O3 2.029(3) Å, Ni1 – O4 2.033(3) Å, O3 – Ni2 – Br2 167.6(1) °, O4 – Ni2 – N2 163.6(1) °. Selected distances and angles for **4**: Cu1 --- Cu2 5.20 Å, Cu1 – Br1 2.396(1) Å, Cu2 – Br2 2.362(1) Å, Cu1 – N1 2.240(2) Å, Cu1 – N2 2.027(2) Å, Cu2 – N3 2.049(2) Å, Cu2 – N4 2.223(2) Å, Cu2 – O3 2.019(2) Å, Cu2 – O4 1.991(2) Å, O2 – Cu2 – N2 171.6(1) °, O4 – Cu2 – N4 132.1(1) °.

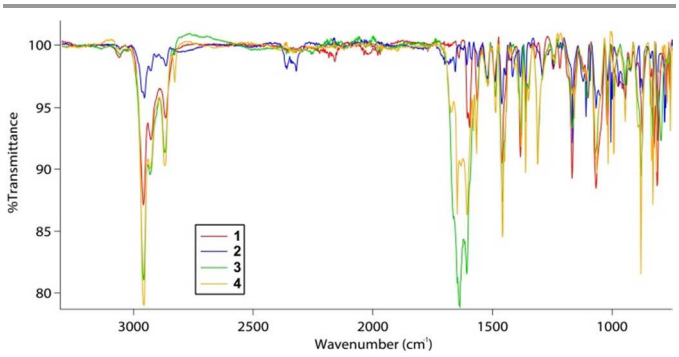

Figure 4. IR spectra of complexes **1**-**4**.

To gain additional information on the nature of compounds **1-4** in solution, we have characterized them by mass spectrometry (ESI-MS). Di-nickel complexes appear to be significantly more stable under MS conditions, allowing the detection of molecular ions. Thus, compound **1** gives rise to the molecular ion peak at m/z 1071.5 that is attributed to the $[Ni_2(L)Br_3]^+$ (**1**-Br) (**Figure S5**). In contrast, no corresponding $[Cu_2(L)Br_3]^+$ (**1**-Br) is observed. Instead, only the monometallic species $[Cu(L)Br]^+$ is detected at m/z 860.3. Compound **3** appears to be particularly stable under MS conditions, giving rise to two prominent peaks consistent with the mono-cation $[Ni_2(L)(C_2O_4)Br]^+$ ([**3**-Br-CH_3CN]) and the di-cation $[Ni_2(L)(C_2O_4)]^{2+}$ ([**3**-2Br-CH_3CN]). To confirm the nature of these ions, we further characterized this compound by high-resolution mass spectrometry, and correlated the obtained spectra with the expected isotopic distribution. The peak at m/z 1001.2656 (**Figure 5**) is consistent with the mono-cation $[Ni_2(L)(C_2O_4)Br]^+$. The peak at m/z 461.1706 is consistent with the di-cation $[Ni_2(L)(C_2O_4)]^{2+}$ (see **Figure S6**).

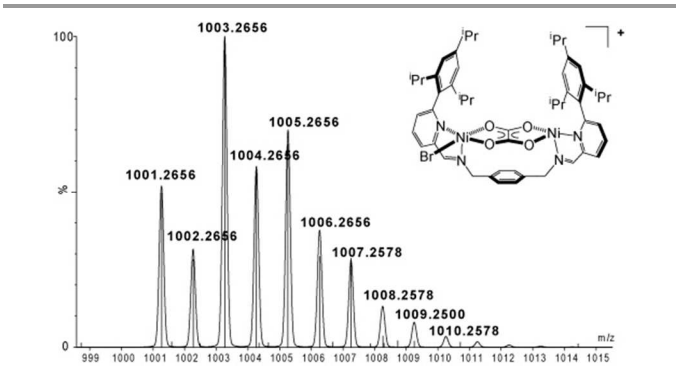

Figure 5. Experimental and calculated ESI-MS spectrum of complex **3** in the 1000-1015 region, demonstrating the peak attributed to [**3**-Br-CH_3CN]$^+$.

As compound **1** demonstrates more significant colour change than compound **2**, and can be easily detected *in situ* by mass spectrometry, we decided to focus on further exploration of its reactivity. The reactivity of **1** is not limited to $(NBu_4)_2[C_2O_4]$ in organic solvents. Addition of MeOH, or MeOH/H_2O (4:1) solutions of either $K_2C_2O_4$ of $Na_2C_2O_4$ to a

1:1 solution of **1** in THF/CH_3CN leads to the formation of green solutions containing **3** (based on mass spectrometry), from which pure **3** can be isolated upon recrystallization. We followed oxalate incorporation using UV-vis spectroscopy. UV-vis spectra of compounds **1** and **3** are presented in **Figure 6**. The spectra (inset) clearly demonstrate significant differences between **1** and **3**. Upon titration of **1** with $(NBu_4)_2[C_2O_4]$ a clean disappearance of **1** and emergence of **3** are observed (**Figure 6**).

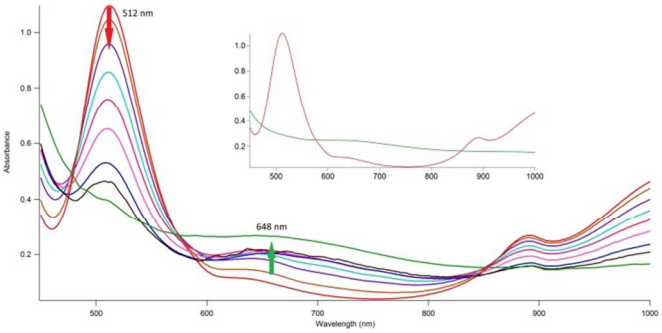

Figure 6. Spectrophotometric titration of **1** with $(NBu_4)_2[C_2O_4]$ in CH_3CN/THF. Inset: Spectrum of the starting material (**1,** red line); spectrum of the product (**3,** green line).

Following our studies on the oxalate binding by complex **1**, we have interrogated the selectivity of **1** for oxalate, versus other simple mono- and di-carboxylates: formate, acetate, succinate, malonate, and glutarate. We decided to use mass spectrometry as a tool to determine selectivity of the di-nickel system **1** toward oxalate, versus other carboxylates, due to several reasons. Most importantly, compound **3** gives rise to an easily recognizable ESI-MS fingerprint at 1001 (highest peak at 1004 in the low-resolution mass spectrum) corresponding to the mono-cation $[Ni_2(L)(C_2O_4)Br]^{1+}$ (**Figure 5**), which allows its easy and reliable detection. In addition, the UV-vis spectra of the products of the reaction of compound **1** with other carboxylates are very similar to that of compound **3** (see **Figures S22-S26** for details). Whereas mass spectrometry does not provide a quantitative tool, it nevertheless allows direct observation of the products of competition experiments given their stability under the analytic conditions.[16] Two series of experiments were conducted. In the first series of experiments, compound **1** was treated with the equimolar amounts of the respective mono- or dicarboxylate (formate, acetate, malonate, succinate, and glutarate). Next, the products of these reactions were analysed by electrospray (ESI) mass spectrometry. The results of these experiments are displayed in **Figure 7**. Only the most significant region (950 – 1100 m/z) is shown in **Figure 7**; full mass spectra are given in supporting information. Mass spectra clearly demonstrate the expected products of the reaction of **1** with the respective carboxylate. The addition of formate gives rise to the two peaks at m/z = 1040 and 1076 ($[Ni_2(L)(O_2CH)Br_2]^{1+}$ and $[Ni_2(L)Br_3]^{1+}$, respectively). Similarly, the reaction of compound **1** with acetate gives rise to the peaks at m/z = 1034, 1056, and 1076, corresponding to $[Ni_2(L)(O_2CCH_3)_2Br]^{1+}$, $[Ni_2(L)(O_2CCH_3)Br_2]^{1+}$ and $[Ni_2(L)Br_3]^{1+}$, respectively. The addition of malonate to the solutions of **1** leads to the signal at m/z = 1017, consistent with $[Ni_2(L)(O_2CCH_2CO_2)Br]^{1+}$. Treatment of **1** with succinate gives rise to the signal at m/z = 1032 ($[Ni_2(L)(O_2C(CH_2)_2CO_2)Br]^{1+}$. The reaction of **1** with glutarate leads to the signal at m/z of 1047, indicating $([Ni_2(L)(O_2C(CH_2)_3CO_2)Br]^{1+}$.

In the second series of experiments, the mixtures of **1** with the respective mono- or dicarboxylates (designated as [**1**+carboxylate] in **Figure 7**) were treated with one equivalent of oxalate; the resulting products were also analysed by ESI-MS (**Figure 8**). Treatment of the solution of [**1**+formate] with oxalate leads to a single signal around m/z = 1004, indicative of the formation of the oxalate complex $([Ni_2(L)(O_2CCO_2)Br]^{1+}$ only. Treatment of the solution of [**1**+acetate] with oxalate leads to the detection of two products in 950-1100 region: $([Ni_2(L)(O_2CCO_2)Br]^{1+}$ (1004) and $([Ni_2(L)(O_2CCO_2)(O_2CCH_3)]^{1+}$ (982). This result is consistent with the previous observation of $[Ni_2(L)Br_3]^{1+}$, $[Ni_2(L)(O_2CCH_3)Br_2]^{1+}$ $[Ni_2(L)(O_2CCH_3)_2Br]^{1+}$ species in the mixture of [**1**+acetate] (**Figure 7**). The reaction of [**1**+malonate] with oxalate forms $([Ni_2(L)(O_2CCO_2)Br]^{1+}$ as the only product detected by mass spectrometry. Treatment of [**1**+succinate] with oxalate leads in the appearance of the prominent oxalate signal at m/z = 1004, although a minor signal attributable to $([Ni_2(L)(O_2C(CH_2)_2CO_2)Br]^{1+}$ is also observed at m/z = 1032. Finally, treatment of [**1**+glutarate] with stoichiometric amounts of oxalate gives rise to the signal at m/z = 1004, although other signals are also detected around m/z = 989 and m/z = 1041. We were not able to assign these signals.

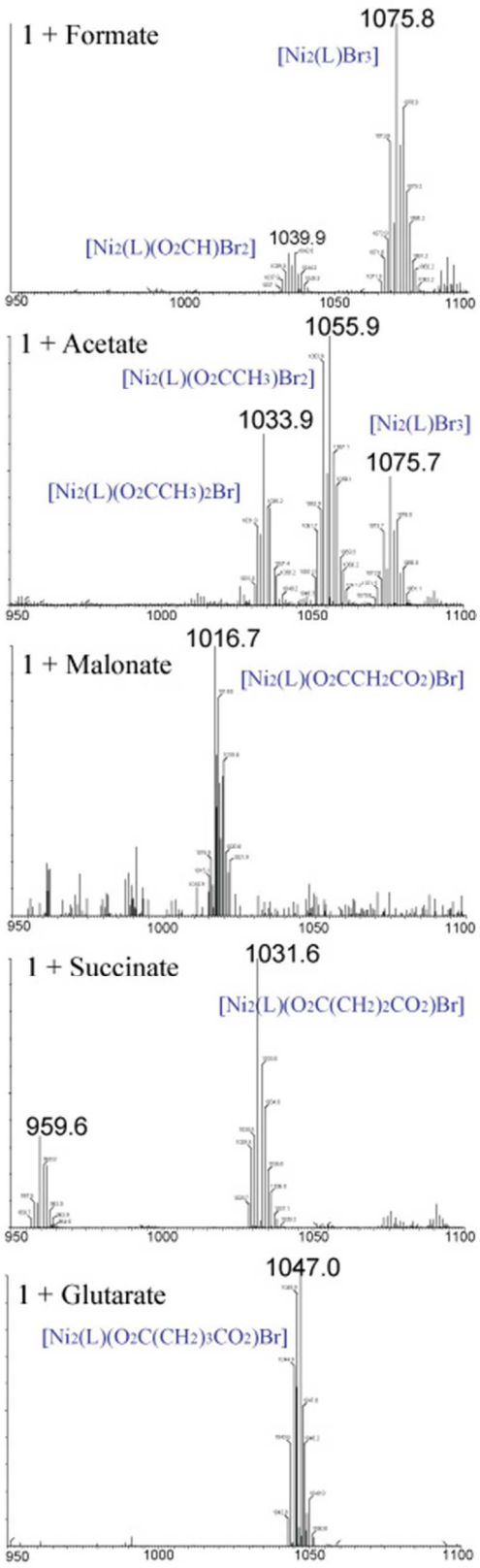

Figure 7. ESI mass spectra (in the range of m/z 950-1100) of the reaction mixtures of complex **1** with formate, acetate, malonate, succinate, and glutarate.

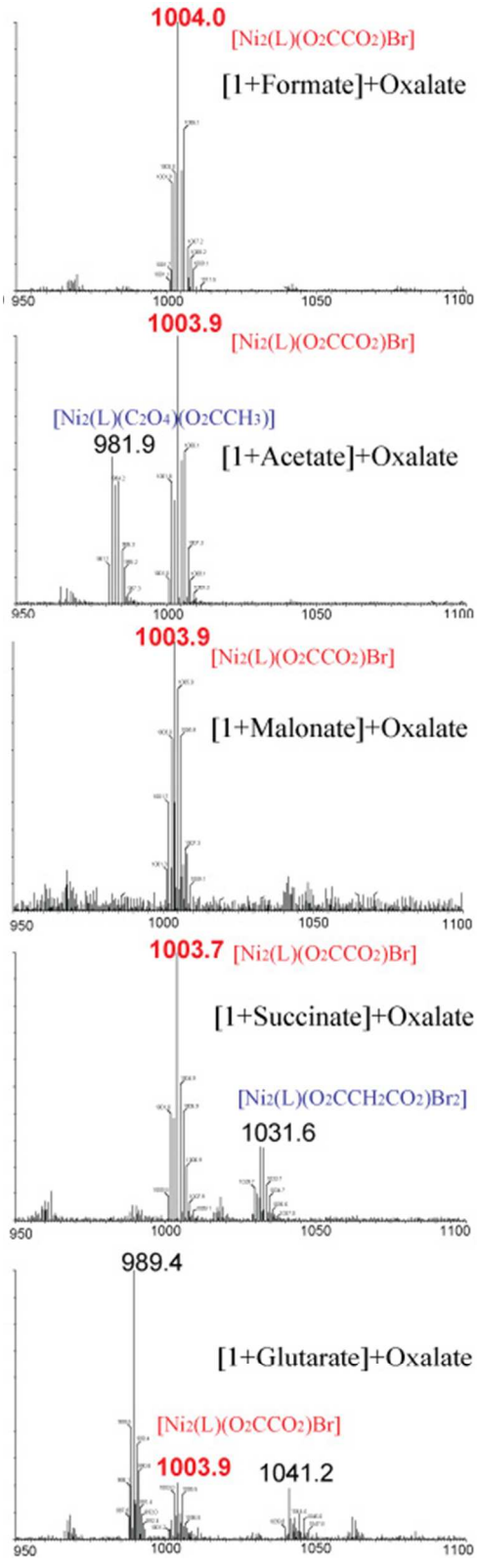

Figure 8. ESI mass spectra (in the range of m/z 950-1100) of the competition experiments involving addition of oxalate to the reaction mixtures of complex **1** with formate, acetate, malonate, succinate, and glutarate.

We have also determined binding affinity of the di-nickel system for oxalate. The binding constant was determined by the spectrophotometric titration of the metal complex (**1**) with oxalate, followed by fitting the data to the non-linear curve as previously described.[17] The obtained binding constant of 5.2 * 10^2 M^{-1} appears to be two to three orders of magnitude lower than those previously reported for the dinuclear complexes.[5-10] It is possible that the significant flexibility of our system is responsible for the decreased value of the binding constant, versus previously reported systems. We surmised that such flexibility may also lead to the reversibility in oxalate coordination within the intra-complex cavity. Thus, we investigated next whether the oxalate can be released from **3**. Toward this goal, compound **3** was treated with slight excess of calcium bromide, as calcium salts are known to form insoluble calcium oxalate.[18] Addition of the colourless acetonitrile solution of $CaBr_2$ (2 equiv) to the stirred green solution of **3** immediately results in the colour change to red and the formation of white precipitate. Recrystallization of the red residue from THF demonstrates that the starting material $Ni_2(L)Br_4$ (**1**) has been restored. Interestingly, **1** co-crystallizes with one equivalent of $CaBr_2(THF)_4$ (**Figure 9**).

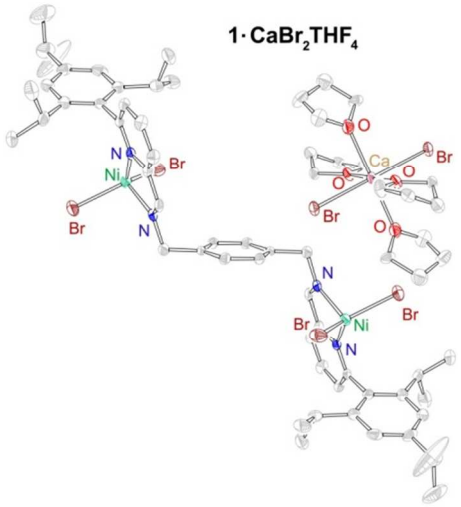

Figure 9. X-ray structure of **1**•$CaBr_2(THF)_4$ (50% probability ellipsoids).

The structure of **1**•$CaBr_2(THF)_4$ demonstrates slightly different relative conformation of metal centres in $Ni_2(L)Br_4$ (Ni --- Ni separation of 10.22 Å). However, bond metrics around Ni centers are overall similar to those in compound **1**. We have also attempted to extract oxalate from compound **4**. The addition of the acetonitrile solution of $CaBr_2$ to compound **4** has also led to the formation of calcium oxalate. However, we were not able to isolate the copper products of this reaction.

Conclusions

We demonstrated that the highly flexible di-nickel and di-copper complexes tethered by an open-chain bis(iminopyridine) ligand bind oxalate in the intramolecular cavity. The di-nickel complex allows colourimetric detection of oxalate as oxalate incorporation is accompanied by a substantial colour change. Oxalate recognition by the di-nickel complex is selective as oxalate replaces other simple mono- and di-carboxylate tested. The highly flexible nature of the system leads to the relatively low oxalate-binding constant compared with other (mostly pre-organized macrocyclic) systems previously reported. However, this flexibility enables reversible incorporation of oxalate, making our sensor recyclable.

Experimental

General methods and procedures

Nickel bromide dimethoxyethane complex ($NiBr_2$(DME)), copper(II) bromide, oxalic acid dihydrate, tetrabutylammonium methoxide solution, potassium oxalate dihydrate, sodium oxalate, ammonium formate, ammonium acetate, succinic acid disodium salt, malonic acid and glutatric acid were purchased from Aldrich, Strem or TCI America and used as received. L has been prepared as previously described.[12c] All solvents were purchased from Fisher scientific and were of HPLC grade. The solvents were purified using an MBraun solvent purification system and stored over 3-Å molecular sieves. Compounds were routinely characterized by ^{1}H NMR spectroscopy, Evans method, X-ray crystallography, IR spectroscopy, elemental analyses, and mass spectrometry (ESI). NMR spectra were recorded at the Lumigen Instrument Center (Wayne State University) on a Varian Mercury 400 NMR Spectrometer in CD_3CN at room temperature. Chemical shifts and coupling constants (*J*) were reported in parts per million (δ) and Hertz respectively. IR spectra of powdered samples were recorded on a Shimadzu IR Affinity-1 FT-IR Spectrometer outfitted with a MIRacle10 attenuated total reflectance accessory with a monolithic diamond crystal stage and pressure clamp. Low resolution mass spectra were obtained at the Lumigen Instrument Center utilizing a Waters Micromass ZQ mass spectrometer (direct injection, with capillary at 3.573 (KV) and cone voltage of 20.000 (V)). Only selected peaks in the mass spectra are reported below. UV-visible spectra were obtained on a Shimadzu UV-1800 spectrometer. Elemental analyses were performed under ambient conditions by Midwest Microlab LLC or Columbia Analytical Services, Inc.

Synthesis and characterization of compounds

Synthesis of $Ni_2(L)Br_4$ (**1**) - To a 3 mL solution of $NiBr_2$DME (17.2 mg, 0.056 mmol) in THF a slurry of L (20.0 mg, 0.028 mmol) in 3 mL of THF was added. The mixture was allowed to stir for one hour. The resulting pink solution was

filtered. The solvent of the filtrate was removed in vacuo. X-ray quality pink crystals were obtained by vapor diffusion of diethyl ether into a concentrated THF/CH_3CN solution yielding 26.0 mg of $Ni_2(L)Br_4$ (**1**, 82%). M.p. 215 °C (decomposition). ESI-MS Calcd for $[C_{50}H_{62}N_4Ni_2Br_3]^+$ (**1** – Br) 1071.1, found 1071.5. Anal. Calcd for $C_{50}H_{62}N_4Ni_2Br_4$: C, 52.0; H, 5.4; N, 4.9. Found: C, 52.3; H, 5.3; N, 5.0. The structure was also confirmed by X-ray structure determination (**Figure 2, Table S1**). ^{1}H NMR (CD_2Cl_2, 400 MHz) δ 1.3, 1.6, 2.9, 10.7, 16.0, 18.9, 45.5, 77.4 ppm. μ_{eff} (Evans, CD_2Cl_2, 298 K): 4.83 μ_B. IR (cm^{-1}): 2956 (s), 1458 (s), 1369 (m), 1170 (m), 1050 (m), 880 (m).

Synthesis of $Cu_2(L)Br_4(CH_3CN)_2$ **(2)** – To a 3 mL solution of $CuBr_2$ (8.0 mg, 0.056 mmol) in THF a slurry of L (20.0 mg, 0.278 mmol) in 3 mL of THF was added. Upon the addition, the color changed to green-yellow. The mixture was allowed to stir for one hour. The solvent was removed under vacuum. X-ray quality green crystals were obtained by vapour diffusion of Et_2O into a concentrated CH_3CN solution yielding $Cu_2(L)Br_4(CH_3CN)_2$ (**2**, 24.0 mg, 75%). M.p. = 90 °C (decomposition). Anal. Calcd. for $C_{54}H_{68}Br_4N_6Cu_2$: C, 51.9; H, 5.5; N, 6.7 Found: C, 51.3; H, 5.4; N, 6.4. ESI-MS Calcd for $[C_{50}H_{62}N_4Cu_2Br_2]^+$ (1- 2Br) 1002.2, found. 1002.6. The structure was confirmed by X-ray structure determination (**Figure 2, Table S1**). μ_{eff} (Evans, CD_2Cl_2, 298 K): 2.16 μB. IR (cm^{-1}): 2956 (s), 2360 (w), 1458 (s), 1369 (m), 1170 (m), 1050 (m), 880 (m).

Synthesis of $(NBu_4)_2[C_2O_4]$ – This procedure is a modification of a previously reported method.[14] To a 20 mL solution of oxalic acid dihydrate (0.500 g, 3.976 mmol) 13.3 mL of $(NBu_4)(OMe)$ (20% in MeOH) solution was added. The reaction was allowed to stir for 4 hours. The solvent was removed under vacuum. The resulting solid was dried under high vacuum for 24 h yielding 2.22g (98%) of $(NBu_4)_2[C_2O_4]$. ^{1}H NMR (CD_3CN, 400 MHz) δ 3.15 (t, *J = 8.0*, 16H), 1.59 (q, *J = 6.4*, 16H), 1.33 (q, *J = 7.2,* 16H), 0.93 (t, *J = 6.8,* 24H),); ^{13}C NMR (CD_3CN, 75 MHz) δ 176.72, 59.20, 24.40, 20.34, 13.87.

Synthesis of $Ni_2(L)(\mu\text{-}C_2O_4)Br_2(NCMe)$ (**3**) – To a 3 mL of solution of **1** (26.3 mg, 0.023 mmol) in THF a 2 mL solution of $(NBu_4)_2[C_2O_4]$ (13.0 mg. 0.023 mmol) in CH_3CN was added, resulting in green solution. The mixture was allowed to stir for one hour, filtered, and the volatiles were removed in vacuo. Green X-ray quality crystals were obtained by slow diffusion of ether into CH_3CN yielding 20 mg of $Ni_2(L)(\mu\text{-}C_2O_4)Br_2(NCMe)$ (**3,** 78%). M.p. = 207 °C (decomposition). ESI-MS Calcd for $[C_{50}H_{62}N_4Ni_2C_2O_4Br]^+$ (**3** – Br – CH_3CN) 1001.3, found 1001.3. Anal. Calcd for $C_{54}H_{65}N_5Ni_2Br_2O_4$: C, 57.6; H, 5.8; N, 6.2. Found: C, 56.6; H, 5.8; N, 6.0. The structure was also confirmed by X-ray structure determination (**Figure 3, Table S1**). IR (cm^{-1}): 2956 (s), 1647 (s), 1607 (s), 1458 (s), 1369 (m), 1310 (m), 1170 (m), 1050 (m), 880 (m).

Synthesis of $Ni_2(L)(\mu\text{-}C_2O_4)Br_2(CH_3CN)$ **(3)** *using NaC_2O_4 or KC_2O_4* – To a 3 mL of solution of **1** (26.0 mg, 0.028 mmol) in THF $K_2C_2O_4{\cdot}2H_2O$ (5.0 mg, 0.028 mmol) in 1 mL of MeOH was added. Upon the addition, the color changed to dark green. The mixture was allowed to stir for 1 h then filtered. The resulting green solution was concentrated under vacuum. Green X-ray quality crystals were obtained by slow diffusion of ether into CH_3CN yielding $Ni_2(L)(\mu\text{-}C_2O_4)Br_2(CH_3CN)$ (18 mg, 72%) as green crystals. The nature of the product was confirmed by the unit cell determination (identical to the unit cell of **3**). The compound **3** can be obtained in a similar fashion using the solution of NaC_2O_4 (3.7 mg. 0.0278 mmol) in a 1:1 mixture of MeOH:H_2O.

Synthesis of $Cu_2(L)(C_2O_4)Br_2$ (**4**) – To a 3 mL of solution of **2** (66 mg, 0.0556 mmol) in CH_3CN a 2 mL solution of $(NBu_4)_2[C_2O_4]$ (32 mg. 0.056 mmol) in CH_3CN was added. Upon the addition, the colour changed to dark green. The mixture was allowed to stir for 1 h then filtered. The resulting green solution was concentrated under vacuum. Green X-ray quality crystals were obtained by slow diffusion of ether into CH_3CN yielding $Cu_2(L)(C_2O_4)Br_2$ (**4**, 50 mg, 83%). M.p. = 152 °C (decomposition). Anal. Calcd. for $C_{52}H_{64}Br_2N_4O_4Cu_2$:C, 57.1 H, 5.7 N, 5.1 Found: C, 57.1 H, 5.7 N, 5.2. The structure was also confirmed by X-ray structure determination (**Figure 3, Table S1**). IR (cm^{-1}): 2956 (s), 1647 (s), 1607 (s), 1458 (s), 1369 (m), 1310 (m), 1170 (m), 1050 (m), 880 (m).

Oxalate extraction from $Ni_2(L)(\mu\text{-}C_2O_4)Br_2(CH_3CN)$ **(3)** *to form $Ni_2(L)Br_4{\bullet}CaBr_2THF_4$* (**1•CaBr$_2THF_4$**) – To a green 3 mL of solution of **3** (12 mg, 0.011 mmol) in CH_3CN a colourless 2 mL solution of $CaBr_2$ in CH_3CN (4 mg. 0.02 mmol) was added. The reaction color immediately turned red-pink, and white precipitate formed. The mixture was allowed to stir for 1 h then filtered. The resulting red-pink solution was concentrated under vacuum. Pink x-ray quality crystals were obtained by slow diffusion of ether into THF solution yielding $Ni_2(L)Br_4{\bullet}CaBr_2THF_4$ (**1**•$CaBr_2THF_4$, 14 mg, ca. 90%). The nature of the product was established by the X-ray structure determination (**Figure 9**).

General procedure for obtaining the ESI-MS of the products of the reaction of **1** *with mono- and di-carboxylates* – To a solution of L (20 mg, 0.278 mmol) and 2 equiv. $NiBr_2DME$ (17 mg, 0.556 mmol) in THF a mixture of 1 equiv of the corresponding mono- or dicarboxylate ion (formate, acetate, succinate, malonate, and gluratate) in MeOH was added and shaken for 2 min. An aliquot of the resulting solution was then injected into the ESI-MS for analysis.

General procedure for obtaining the electrospray mass spectra of the products of the reaction of **1** *with the mixtures of mono- and dicarboxylates with oxalate* – To a solution of L (20 mg,

0.278 mmol), 2 equiv $NiBr_2DME$ (17 mg, 0.556 mmol) in THF and 1 equiv of the competitor ion (formate, acetate, succinate, malonate, and gluratate) in MeOH a mixture of 1 equiv of $(NBu_4)_2[C_2O_4]$ (16 mg, 0.278 mmol) was added and shaken for 2 min. An aliquot of the resulting solution was then injected into the ESI-MS for analysis.

X-ray crystallographic details

Structures of compounds **1**, **2**, **3**, **4**, and **1**•$CaBr_2(THF)_4$ were confirmed by X-ray structure determination. The crystals were mounted on a Bruker APEXII/Kappa three circle goniometer platform diffractometer equipped with an APEX-2 detector. A graphic monochromator was employed for wavelength selection of the Mo Kα radiation (λ = 0.71073 Å). The data were processed and refined using the APEX2 software. Structures were solved by direct methods in SHELXS and refined by standard difference Fourier techniques in the SHELXTL program suite (6.10 v., Sheldrick G. M., and Siemens Industrial Automation, 2000). Hydrogen atoms were placed in calculated positions using the standard riding model and refined isotropically; all other atoms were refined anisotropically. Some of the para-iPr groups displayed large wagging motion which in selected cases (1) was successfully modelled as two different conformations. In contrast, we had only limited success in modelling the disorder of the para-iPr groups in the structures of **2** and **3**. Even though these structures were collected at 100K the thermal parameters for some of these groups were very high. The conclusion is that these groups are not well defined and thus some were refined isotropically. The isotropic refinement of these atoms does not significantly alter the R-factor, and does not alter the conclusions of this paper in any way. Structures of **3** and **4** contained one molecule of ether solvent, and one molecule of acetonitrile in the asymmetric unit. Structure of **1**•$CaBr_2(THF)_4$ contained one molecule of ether solvent in the asymmetric unit. The acetonitrile ligands in the structures of **2** and **3** were disordered over two positions. In addition, the structure of **2** contained acetonitrile solvent disordered over two positions in the asymmetric unit. Detailed crystal and structure refinement data are given in **Table S1**.

Acknowledgements

We thank Wayne State University for startup funding, Dr. Lew Hryhorczuk and Dr. Yuriy Danylyuk for the experimental assistance. JWB thanks the Department of Chemistry for the Continuing Graduate Rumble Fellowship. DSW thanks Undergraduate Research Opportunities Program of Wayne State University for the Undergraduate Research and Creative Projects Award.

Notes and references

[a] Department of Chemistry, Wayne State University, Detroit, Michigan 48202, USA. E-mail: groysman@chem.wayne.edu

Electronic Supplementary Information (ESI) available: crystallographic data in CIF format, mass spectra, NMR spectra, UV-vis spectra, and details on the determination of oxalate binding constant for **3**. CCDC 987904 – 987906, 987908 - 987909. See DOI: 10.1039/b000000x/

1 (a) D. Svedružić, S. Jónsson, C. G. Toyota, L. A. Reinhardt, S. Ricagnoc, Y. Lindqvist, and N. G. J. Richards, *Arch. Biochem. Biophys*., 2005, **433**, 1776. (b) E. L. Greene, G. Farell, S. H. Yu, T. Matthews, V. Kumar, and J. C. Lieske, *Urol. Res*., 2005, **33**, 340. (c) I. A. Al-Wahsh, H. T. Harry, R. G. Palmer, M. B. Reddy, and L. K. Massey, J. *Agric. Food Chem*., 2005, **53**, 5670.

2. (a) M. Gruselle, C. Train, K. Boubekeur, P. Gredin, and N. Ovanesyan, *Coord. Chem. Rev*., 2006, **250**, 2491. (b) F. Abraham, B. Arab-Chapelet, M. Rivenet, C. Tamain, and S. Grandjean, *Coord. Chem. Rev*., 2013, In Press. (c) M. Clemente-León, E. Coronado, C. Martí-Gastaldo, and F. M. Romero, *Chem. Soc. Rev*., 2011,**40**, 473.

3. CSD search revealed 1186 structures of metal complexes bridged by oxalate. In only 7 structures the metals were linked by dinucleating ligands (other than oxalate).

4. S. P. Foxon, O. Walter, R. Koch, H. Rupp, P. Müller, and S. Schindler, *Eur. J. Inorg. Chem.,* 2004, 344.

5. M. Hu, and G. Feng, *Chem. Commun.,* 2012, **48**, 6951.

6. M. M. Rhaman, F. R. Fronczek, D. R. Powell, and M. A. Hossain, *Dalton Trans*., **2014**, DOI: 10.1039/C3DT53467G

7. L. Tang, J. Park, H.-J. Kim, Y. Kim, S. J. Kim, J. Chin, and K. M. Kim, *J. Am. Chem. Soc*., 2008, **130**, 12606.

8. P. Mateus, R. Delgado, P. Brandão, and V. Félix, *Chem. Eur. J*., 2011, **17**, 7020.

9. C. Männel-Croisé, C. Meister, and F. Zelder, *Inorg. Chem*., 2010, **49**, 10220.

10. L. - J. Tang, and M.-H. Liu, *Bull. Korean Chem. Soc.* 2010, **31**, 3159.

11. For selected recent references on the design of dinucleating and multinucleating ligands, see: (a) G. E. Alliger, P. Müller, L. H. Do, C. C. Cummins, and D. G. Nocera, *Inorg. Chem*., 2011, **50**, 4107; (b) D. E. Herbert, and O. V. Ozerov *Organometallics,* 2011, **30**, 6641. (c) T. C. Davenport, and T. D. Tilley, *Angew. Chem. Int. Ed*., 2011, **50**, 12205. (d) D. Huang, and R. H Holm, *J. Am. Chem. Soc*., 2010, **132**, 4693. (e) A. M. Lilio, K. A. Grice, and C. P. Kubiak, *Eur. J. Inorg. Chem*., 2013, 4016. (f) M. R. Radlauer, M. W. Day, T. Agapie, *Organometallics,* 2012, **31**, 22318. (g) A. R. Fout, D. J. Xiao, Q. Zhao, T. D. Harris, E. R. King, E. V. Eames, S. Zheng, and T. A. Betley, *Inorg. Chem*., 2012, **19**, 10290. (h) W. Zhou, N. I. Saper, J. P. Krogman, B. M. Foxman, and C. M. Thomas, *Dalton Trans*., 2014, **43**, 1984.

12. (a) A. Bheemaraju, R. L. Lord, P. Müller, and S. Groysman, *Organometallics*, 2012, **31**, 2120; (b) A. Bheemaraju, J. W. Beattie, R. L. Lord, P. D. Martin, and S. Groysman, *Chem. Commun.,* 2012, **48**, 9595; (c) A. Bheemaraju, J. W. Beattie, E. G. Tabasan, P. D. Martin, R. L. Lord, and S. Groysman, *Organometallics,* 2013, **32**, 2952.

13. Similar dinucleating bis(iminopyridine) ligands lacking bulky groups in the 2' positions led to formation of polymeric materials upon oxalate incorporation. Z. - H. Zhang, S. - C. Chen, M. - Y. He, C. Li, Q. Chen, and M. Du, *Cryst. Growth Des.,* 2011, **11**, 5171.

14. F. A. Cotton, C. Lin, and C. A. Murillo, *J. Chem. Soc., Dalton Trans.: Inorg. Chem.*, 1998, **19**, 3151.
15. http://webbook.nist.gov/chemistry/
16. Mass spectrometry has been previously applied to determine selectivity and ligand/metal binding in solution. For example, see: (a) S. Blasco, M. I. Burguete, M. P. Clares, E. García-España, J. Escorihuela, and S. V. Luis, *Inorg. Chem*., 2010, **49**, 7841. (b) I. Martí, A. Ferrer, J. Escorihuela, M. I. Burguete, and S. V. Luis, *Dalton Trans*., 2012, **41**, 6764.
17. P. Thordarson, *Chem. Soc. Rev*., 2011, **40**, 1305.
18. J. A. Molzon, J. M. Lausier, and A. N. Paruta, *J. Pharm. Sci.,* 1978, **67**, 733.

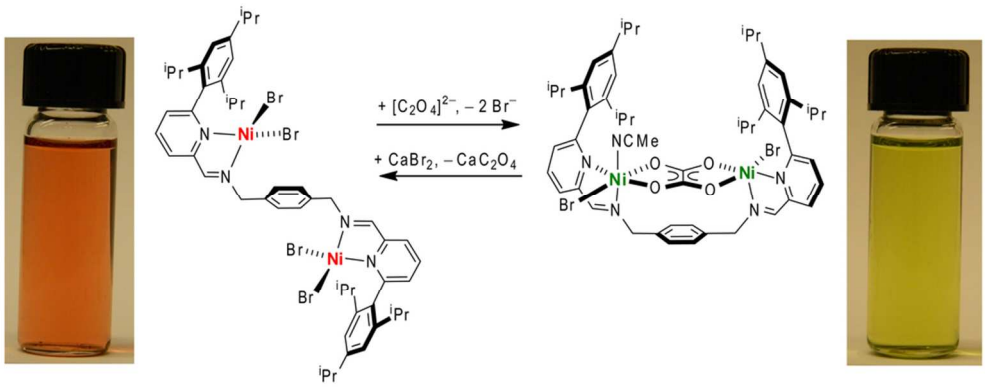

91x34mm (300 x 300 DPI)